Acta Crystallographica Section F
**Structural Biology and Crystallization Communications**
ISSN 1744-3091

# Purification, crystallization and preliminary X-ray analysis of human histidine decarboxylase

**Hirofumi Komori,[a,b]* Yoko Nitta,[c] Hiroshi Ueno[d] and Yoshiki Higuchi[a,b]**

[a]Department of Life Science, Graduate School of Life Science, University of Hyogo, 3-2-1 Koto, Kamigori-cho, Ako-gun, Hyogo 678-1297, Japan, [b]RIKEN SPring-8 Center, 1-1-1 Koto, Mikazuki-cho, Sayo-gun, Hyogo 679-5248, Japan, [c]Graduate School of Human Science and Environment, University of Hyogo, Hyogo 670-0092, Japan, and [d]Laboratory of Applied Microbiology and Biochemistry, Nara Women's University, Kitauoya-nishi-machi, Nara 630-8506, Japan

Correspondence e-mail: komori@sci.u-hyogo.ac.jp

Received 7 March 2012
Accepted 11 April 2012



The core domain of a human histidine decarboxylase mutant was purified and cocrystallized with the inhibitor L-histidine methyl ester. Using synchrotron radiation, a data set was collected from a single crystal at 100 K to 1.8 Å resolution. The crystal belonged to space group $C2$, with unit-cell parameters $a$ = 215.16, $b$ = 112.72, $c$ = 171.39 Å, $\beta$ = 110.3°. Molecular replacement was carried out using the structure of aromatic L-amino-acid decarboxylase as a search model. The crystal contained three dimers per asymmetric unit, with a Matthews coefficient ($V_M$) of 3.01 Å$^3$ Da$^{-1}$ and an estimated solvent content of 59.1%.

## 1. Introduction

Histamine is a bioactive amine responsible for a variety of physiological reactions, including allergies (Galli *et al.*, 2008), gastric acid secretion (Andersson *et al.*, 1998) and neurotransmission (Nuutinen & Panula, 2010). In mammals, the production of histamine from histidine is catalyzed by histidine decarboxylase (HDC; EC 4.1.1.22). HDC is the rate-limiting enzyme in histamine biosynthesis, and HDC-knockout mice are nearly devoid of histamine (Ohtsu *et al.*, 2001).

Mammalian HDC is a pyridoxal 5′-phosphate (PLP)-dependent decarboxylase and belongs to the same family as mammalian glutamate decarboxylase (GAD) and mammalian aromatic L-amino-acid decarboxylase (AroDC) (Sandmeier *et al.*, 1994). The decarboxylases of this family function as homodimers and catalyze the formation of physiologically important amines such as $\gamma$-aminobutyric acid (GABA), dopamine and serotonin *via* the decarboxylation of glutamate, 3,4-dihydroxyphenylalanine (DOPA) and 5-hydroxytryptophan, respectively. Despite their high sequence homology, AroDC and HDC react with different substrates. For example, AroDC catalyzes the decarboxylation of several aromatic L-amino acids, but has little activity towards histidine. Although these differences are known, the substrate specificity of HDC has not been extensively studied because of the low levels of HDC in the body and the instability of recombinant HDC, even in a well purified form (Olmo *et al.*, 2002). However, knowledge of the substrate specificity and decarboxylation mechanism of HDC is valuable from the viewpoint of drug development, as it could help lead to the design of novel drugs to prevent histamine biosynthesis.

The structure of mammalian histidine decarboxylase has not yet been reported. Its three-dimensional structure will provide invaluable insights into the molecular basis of its histidine substrate specificity. To understand the molecular basis of HDC catalysis and specificity, we purified and crystallized a human HDC (hHDC) core-domain mutant. Here, we report the purification, crystallization and preliminary X-ray diffraction analysis of the hHDC core domain as the first step towards structure determination.

## 2. Materials and methods

### 2.1. Site-directed mutagenesis, expression and purification

To define the core domain of hHDC, the amino-acid sequence (662 amino acids) was aligned with those of 2 group II decarboxylases, namely GAD (Fenalti *et al.*, 2007) and AroDC (Burkhard *et al.*, 2001), using the program *ClustalW* (http://www.ebi.ac.uk/clustalw/).

On the basis of this analysis, the core domain of hHDC was determined to extend from the N-terminus to residue 477. This domain was cloned and expressed in *Escherichia coli*. The core domain was amplified by PCR using *Pfu* DNA polymerase. The set of primers used for the amplification were HDC-F (5′-ACGC**GGATCC**ATG-ATGGAGCCTGAGGAGTAC-3′; the *Bam*HI restriction site is shown in bold) and HDC-R (5′-ACCG**CTCGAG**TTACTGACTC-AGGATGAGAGTG-3′; the *Xho*I restriction site is shown in bold). The hHDC cDNA was obtained from the plasmid previously constructed for the expression of hHDC in *E. coli* (Nitta *et al.*, 2010). The PCR product was cloned into the pGEX-6p-1 plasmid between the *Bam*HI and *Xho*I sites. The core domain of hHDC carrying double mutations, C179S and C417S, was constructed by PCR using the QuikChange Site-Directed Mutagenesis kit (Stratagene). The oligonucleotides used for the mutagenesis were as follows: C179S, 5′-CCGATGCTGATGAGTCCTCCCTAAATGCCCG-3′ and 5′-CGGGCATTTAGGGAGGACTCATCAGCATCGG-3′; C417S, 5′-GGTTTTTCGTCTAAAGGGTCCTAATTCTCTCACA-GAAAATG-3′ and 5′-CATTTTCTGTGAGAGAATTAGGACCCTT-TAGACGAAAAACC-3′. The correct nucleotide sequence of the constructs was confirmed by DNA sequencing (Hokkaido System Science Co. Ltd).

Transformed *E. coli* Rosetta 2 (DE3) cells bearing the constructs were grown at 298 K in Luria–Bertani (LB) medium supplemented with ampicillin (50 mg ml$^{-1}$) and chloramphenicol (10 mg ml$^{-1}$). The cells were collected by centrifugation and resuspended in 50 m*M* phosphate buffer pH 6.8 plus 300 m*M* NaCl, 1% polyethylene glycol (PEG) 300 and 10 µ*M* PLP. After cell disruption by sonication, the lysates were centrifuged at 20 000*g* for 60 min. The supernatant was loaded onto a glutathione column and the GST tag was cleaved with PreScission protease (16 h at 277 K). Subsequently, the PreScission-treated sample was applied onto a second glutathione column to sequester uncleaved protein. The flowthrough fraction was loaded onto a Resource Q column pre-equilibrated with 50 m*M* Tris pH 8.0. The column was washed with the same buffer and eluted with a linear gradient of 0–250 m*M* NaCl at a flow rate of 2 ml min$^{-1}$. Fractions containing the hHDC core domain were pooled for additional purification using a Superdex 200 gel-filtration column (GE Healthcare) with 20 m*M* HEPES buffer pH 7.0, 100 m*M* NaCl. The purity of the final protein preparation was evaluated by 10% SDS–PAGE. Fractions containing the hHDC core domain were pooled and concentrated to 10 mg ml$^{-1}$ using a Vivaspin 20 (30 kDa molecular-weight cutoff).

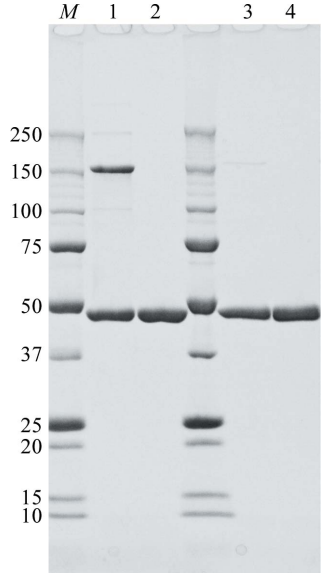


**Figure 1**
Nonreducing SDS–PAGE gel of recombinant hHDC core domains. Lane 1, WT; lane 2, double mutant (C179S and C417S); lane 3, WT with 100 m*M* dithiothreitol (DTT); lane 4, double mutant with 100 m*M* DTT. Lane *M* contains molecular-weight standards (Precision Plus Protein Unstained Standards, Bio-Rad; labelled in kDa). Lane 2 shows the oligomeric states (dimer and trimer) of the hHDC core domain.

### 2.2. Protein crystallization

For crystallization, 0.1 m*M* PLP and 2 m*M* L-histidine methyl ester were added to the hHDC core-domain solution. Crystallization was performed in CrystalClear Strips (Hampton Research) using the sitting-drop vapour-diffusion technique. For initial screening of the crystallization conditions, protein droplets prepared by mixing 1 µl protein solution and 1 µl reservoir solution were equilibrated against 80 µl reservoir solution. Initial crystallization screening was performed using commercially available screening kits from Hampton Research (Index) and Emerald BioSystems (Wizard III and IV and Precipitant Synergy) at 293 K. The conditions were then optimized by varying the PEG concentration and the pH of the buffer. The growth of the crystals was monitored periodically with an optical microscope.

### 2.3. Data collection and crystallographic analysis

An X-ray diffraction data set was collected at 100 K on beamline BL44XU (λ = 0.9000 Å) at SPring-8 using an MX225HE CCD detector. The crystal-to-detector distance was maintained at 175 mm, with an oscillation range of 0.5° per image, covering a total oscillation range of 180°. The unit-cell parameters were determined and the

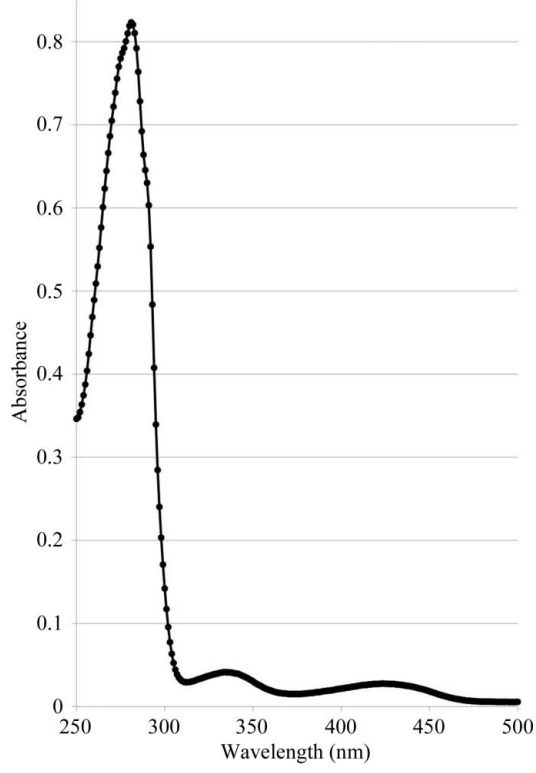


**Figure 2**
Absorption spectrum of the purified hHDC core domain double mutant. The absorption peaks at 335 and 423 nm typical of bound PLP are clearly visible.

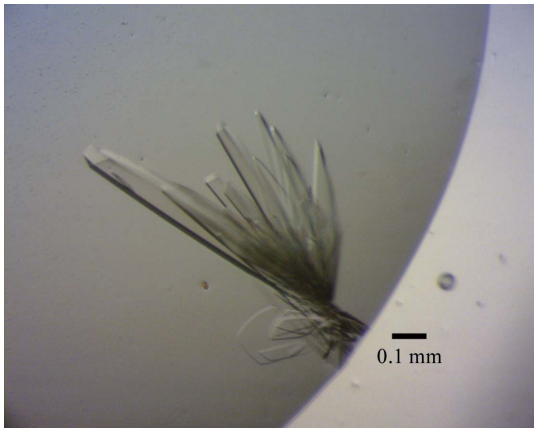


**Figure 3**
Typical crystals of the hHDC core domain double mutant. The maximum crystal dimensions were 0.05 × 0.1 × 0.5 mm.

reflections were integrated using the *HKL*-2000 program package (Otwinowski & Minor, 1997).

## 3. Results and discussion

SDS–PAGE analysis of the purified wild-type (WT) hHDC core-domain sample in the absence of reducing agents revealed several bands with apparent molecular weights (100 and 150 kDa) higher than that of the hHDC core-domain monomer, indicating oligomerization (Fig. 1). Formation of the oligomeric species was possibly mediated *via* disulfide linkages between the free cysteine residues on the surface of each monomer. It was therefore necessary to replace the surface-exposed cysteines with an inert residue in order to prevent aggregation of the recombinant hHDC core domain during crystallization trials. We prepared a double mutation in which Cys179 and Cys417 were replaced by Ser (C179S and C417S); this double mutation prevented nonspecific polymerization and improved the homogeneity. Subsequent gel-filtration analysis indicated that both the wild-type and mutant proteins formed dimers in solution.

The UV–Vis absorption spectrum indicated that the cofactor PLP was bound *via* a Schiff base at the active-site lysine in the hHDC core-domain double mutant (Fig. 2). We attempted crystallization of the hHDC core-domain double mutant in complex with an inhibitor, L-histidine methyl ester, and obtained usable crystals. The crystallization conditions of the hHDC core-domain double mutant were refined and the best crystals of the hHDC core domain were grown using a reservoir solution composed of 28%(*w*/*v*) PEG 3350, 100 m*M* Tris–HCl buffer pH 8.5, 200 m*M* lithium sulfate (Fig. 3). For data collection, the crystals were soaked in a cryoprotectant solution (30% PEG 3350, 100 m*M* Tris–HCl buffer pH 8.5, 200 m*M* lithium sulfate, 10% glycerol) for a few minutes prior to cooling in a nitrogen cold stream at 100 K. The diffraction from the hHDC core-domain double-mutant crystal extended to 1.8 Å resolution. It belonged to space group *C*2, with unit-cell parameters $a$ = 215.16, $b$ = 112.72, $c$ = 171.39 Å, $\beta$ = 110.3°. The data-collection statistics are summarized in Table 1. Calculation of the Matthews coefficient (Matthews, 1968) suggested the presence of three or four dimers in the asymmetric unit. Molecular replacement was carried out by *Phaser* (McCoy *et al.*, 2005) using the AroDC structure (Burkhard *et al.*, 2001) as a model. A good molecular-replacement solution (LLG = 3372) was obtained when three dimers were expected in the asymmetric unit ($V_M$ = 3.01 Å$^3$ Da$^{-1}$; 59.1% solvent content). Further structure refinement is now under way.

**Table 1**
Summary of crystallographic data.

Values in parentheses are for the outer resolution shell.

| | |
|---|---|
| Space group | *C*2 |
| Unit-cell parameters (Å, °) | $a$ = 215.16, $b$ = 112.72, $c$ = 171.39, $\beta$ = 110.3 |
| Resolution (Å) | 50.00–1.80 (1.83–1.80) |
| Total No. of reflections | 1343710 |
| No. of unique reflections | 354047 |
| Multiplicity | 3.8 (3.8) |
| Completeness (%) | 100.0 (100.0) |
| $\langle I/\sigma(I)\rangle$ | 16.0 (2.6) |
| $R_{merge}$ (%) | 6.5 (68.0) |

We thank the staff at beamline BL44XU, SPring-8, Japan. The MX225-HE (Rayonix) CCD detector at BL44XU was financially supported by Academia Sinica and by the National Synchrotron Radiation Research Center (Taiwan, ROC). This work was partly supported by the Kawanishi Memorial ShinMaywa Education Foundation and by a Grant-in-Aid for Young Scientists (B) from the Japan Society for the Promotion of Science.

## References

Andersson, K., Chen, D., Mattsson, H., Sundler, F. & Håkanson, R. (1998). *Yale J. Biol. Med.* **71**, 183–193.
Burkhard, P., Dominici, P., Borri-Voltattorni, C., Jansonius, J. N. & Malashkevich, V. N. (2001). *Nature Struct. Biol.* **8**, 963–967.
Fenalti, G. *et al.* (2007). *Nature Struct. Mol. Biol.* **14**, 280–286.
Galli, S. J., Tsai, M. & Piliponsky, A. M. (2008). *Nature (London)*, **454**, 445–454.
Matthews, B. W. (1968). *J. Mol. Biol.* **33**, 491–497.
McCoy, A. J., Grosse-Kunstleve, R. W., Storoni, L. C. & Read, R. J. (2005). *Acta Cryst.* D**61**, 458–464.
Nitta, Y., Ohshita, J., Liu, H., Kuronuma, Y. & Ueno, H. (2010). *J. Biol. Macromol.* **10**, 73–82.
Nuutinen, S. & Panula, P. (2010). *Adv. Exp. Med. Biol.* **709**, 95–107.
Ohtsu, H. *et al.* (2001). *FEBS Lett.* **502**, 53–56.
Olmo, M. T., Sánchez-Jiménez, F., Medina, M. A. & Hayashi, H. (2002). *J. Biochem.* **132**, 433–439.
Otwinowski, Z. & Minor, W. (1997). *Methods Enzymol.* **276**, 307–326.
Sandmeier, E., Hale, T. I. & Christen, P. (1994). *Eur. J. Biochem.* **221**, 997–1002.